THE CONSTRUCTION AND CHARACTERIZATION OF THE NIST-4 PERMANENT MAGNET SYSTEM

**Leon S. Chao, Frank Seifert, Shisong Li,
Darine Haddad, Stephan Schlamminger, and Jon R. Pratt
Fundamental Electrical Measurements Division
National Institute of Standards and Technology
Gaithersburg, MD, USA**

ABSTRACT

A watt balance is an electromagnetic force balancing instrument to realize the unit of mass at the kilogram level. The magnet system is one of the key components. Our group at the National Institute of Standards and Technology is currently building a next-generation, permanent-magnet driven watt balance, NIST-4. We describe the construction of the magnet system, characterization of the field profile, and adjustment methods used to achieve an ideal magnetic field profile. Although the absolute field strength is not critical, the uniformity of the magnetic flux profile through the air gap of the magnet is essential for a watt balance experiment.

INTRODUCTION

A redefinition of the International System of Units, the SI, is impending and may occur as early as 2018. Specifically, in the context of mass metrology, the base unit kilogram will be redefined in terms of Planck's constant, severing its current ties to the International Prototype Kilogram (IPK). Currently, the NIST-4 watt balance is under construction and will be used to realize the unit of mass in the United States.

THE MAGNET SYSTEM DESIGN

The design of the NIST-4 magnet system was inspired by the BIPM watt balance group. Two opposing Sm_2Co_{17} segmented rings are housed inside a 60 cm diameter 1021 steel yoke. The magnetic circuit guides the field such that an almost azimuthally uniform field permeates through a 3 cm wide, 10 cm tall air gap defined by the inner and outer yokes.

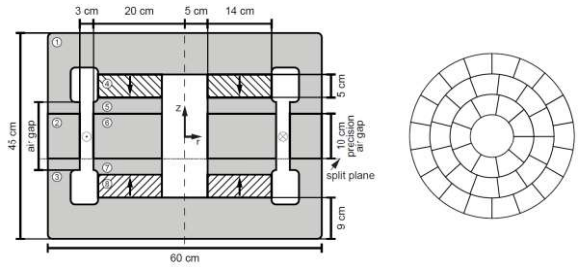

FIGURE 1. Left: a cross sectional view of the magnet system. The circles in the air gap represent the current in the coil and the arrows indicate the direction of magnetization. Right: top view of the segmentation of a Sm_2Co_{17} disk.

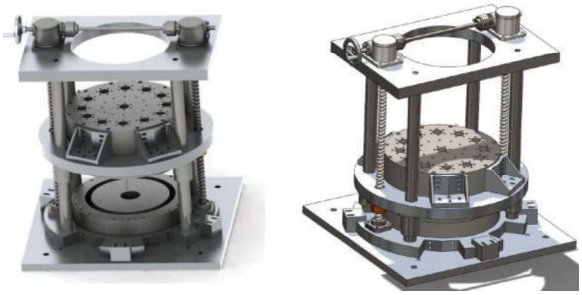

FIGURE 2. To insert the coil into the magnet, it is cranked open with a splitter device. Left: the top two-thirds are removed from the bottom third, exposing the internal air gap. Right: magnet in the closed position.

While NIST was responsible for the conceptual design of the magnet system, the manufacturing was contracted to Electron Energy Corporation[1] (EEC) with a specified field strength of 0.5 Tesla and a "flat profile" uniformity of ±0.01%, or $\Delta B_r/B_r < 2 \times 10^{-4}$. Sm_2Co_{17} is used for the active magnetic material. In order to magnetize the Sm_2Co_{17}, each ring is broken up in 40 sectors. Each 1 kg

[1] Certain commercial equipment, instruments, or materials are identified in this paper in order to specify the experimental procedure adequately. Such identification is not intended to imply recommendation or endorsement by the National Institute of Standards and Technology, nor is it intended to imply that the materials or equipment identified are necessarily the best available for the purpose

segment was sintered and magnetized by a capacitor bank individually.

For each of the 80 segments, the flux characteristics were measured and recorded. The position of every segment was then carefully chosen such that the resulting azimuthal and orthogonal fields were as similar as possible. Post-assembly measurements indicated the two magnet disks were within 0.2 % of each other.

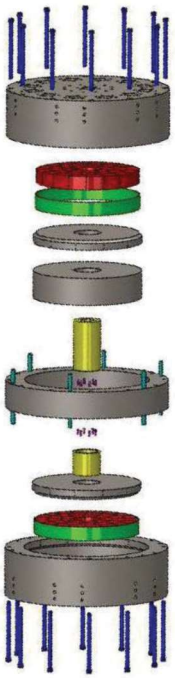

FIGURE 3. Exploded view of the magnet system. The 1021 steel yokes are shaded in light grey and the Sm2Co17 disks are comprised of 40 individually magnetized wedges. The centering tubes are made from stainless steel and their purpose is to keep all the internal components concentric. Dowel pins maintain outer yoke alignment and steel screws lock the assembly together. Stainless steel retaining rings constrain the magnet wedges in the radial direction.

To facilitate the assembly process and to control the repulsive forces between segments, vacuum compatible epoxy was used to secure the magnet segments to the inner yoke plate while a steel retaining ring constricted them radially. A precision ground inner and outer yoke are bound by two identical outer yoke lids, providing the closed magnetic field circuit. Twelve holes on the top and bottom face allow access for hanging an inductance coil inside the precision air gap.

In order to insert the coil, a magnet splitting device was designed. Such a contraption must be able to constrain the unstable state once the magnet has been split and maintain vertical alignment. Each of the four 5 cm diameter steel guide rods is coupled with a frelon-coated linear bearing. The top and bottom yokes are bolted to the magnet splitter frame. Cranking a synchronized set of twin 1/64 gear reducers slowly rotates two lead screws, gradually separating the magnet and providing access to the internal air gap.

METHODS OF CHARACTERIZATION

Two methods were implemented in searching for an unwanted vertical magnetic flux gradient in the air gap: a hall probe and a gradiometer coil (GMC). Both EEC and NIST conducted initial independent hall probe measurements by scanning an 80 mm vertical sweep through each of the 12 access holes (Lakeshore MMZ-2518-UH and HMMT-6704-VR for the EEC and NIST system, respectively). EEC conducted similar hall probe measurements on two different days spaced 1.5 weeks apart (Fig. 4). They measured each access hole at 7 different heights inside the air gap. We measured each access hole continuously by attaching the hall probe to a motorized vertical translation stage.

The gradiometer coil, mean diameter of 433 mm, consisted of two concentric coils wound in series opposition. They are displaced vertically but wound on a single former. A motor driven translation stage moved the coil through the air gap at a constant 2 mm/s. One voltmeter measured the induced voltage of one coil, another the difference, which was used to calculate the gradient of the radial flux density along the vertical.

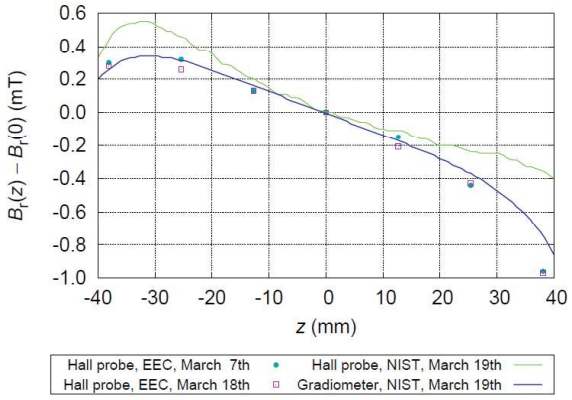

FIGURE 4. EEC and NIST hall probe/gradiometer coil measurements after the initial assembly. All four measurements indicate an approximate -13 μT/mm gradient.

All four measurements were in good agreement, with their mean values differing by about 4 mT (< 8 parts per thousand) (Fig. 4). Each data point is comprised of averaging all 12 holes at the specified z location. The field slopes are all

approximately -13 μT/mm, about a factor of 10 larger than the desired field uniformity. These initial measurements also indicate a variation in the radial flux density of at least 1 mT, failing the requirement of $\Delta B_r/B_r < 2 \times 10^{-4}$. Hence, field profile tuning adjustments were necessary.

FIELD PROFILE ADJUSTMENT

Two methods were attempted to fine-tune the field profile: (1) regrinding the outer middle yoke to make a 0.05 degree taper of the air gap geometry, and (2) introduce a tilt separation between the top two-thirds and bottom third of the magnet to increase the reluctance in the bottom yoke.

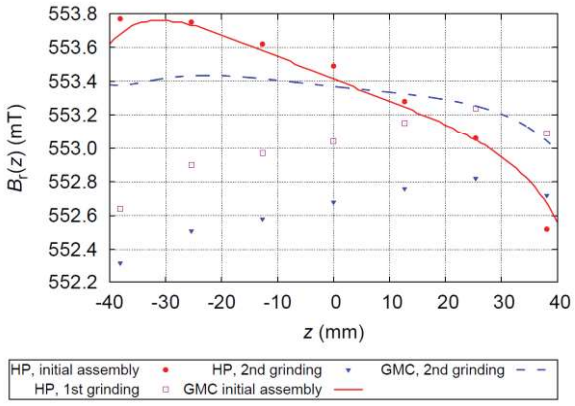

FIGURE 5. These data points represent the magnetic field measured with the hall probe and gradiometer coil before and after regrinding.

REDGRINDING THE OUTER YOKE

The method of regrinding the outer middle yoke (part number 2 in Fig. 1) was to add a slight taper to the air gap such that the top gap is nominally 3.000 cm wide and the bottom is 3.008 cm wide. After regrinding, EEC measured again the field profile to discover the grinding process overshot by 50%, resulting in a slope change from -13 μT/mm to +7 μT/mm. The outer middle yoke was sent back for a second regrinding, this time with the instruction to grind the gap with a less aggressive taper, 3.003 cm at the top and 3.008 cm at the bottom. This procedure failed to indicate any change; the first grinding and the second grinding showed the same gradient. Fig. 5 shows the results of the initial assembly, the first grinding and the second grinding.

From this, we decided to abandon the hall probe measurement setup. It is likely that the translation of the hall probe(s) were not purely vertical and/or nonlinear. For example, if the measurement setup was to blame, the "vertical" probe trajectory would only need a parasitic horizontal component of 0.24 mm over a path length of 80 mm to measure a 7 μT/mm gradient. While the probe was certainly positioned better than 1 mm in the center of the gap, an accuracy of 0.2 mm could not be ensured. After the second regrinding, another GMC measurement was taken, showing a -3.5 μT/mm gradient [2].

SEPARATION METHOD

Since the grinding process proved ineffective, other options were explored. A separation method was implemented, i.e. a gap between the bottom third of the magnet and the top two-thirds was introduced. We found that a flat profile was achieved when the separation was approximately 0.5 mm high. A stable and uniform azimuthal air gap can be maintained by inserting aluminum shim stock pieces at several azimuthal locations.

This separation increases the reluctance in the lower yoke. Hence, the lower Sm_2Co_{17} magnet contributes less flux to the radial field through the precision air gap. While this azimuthal air gap helped achieve the desired flat profile, it also introduced a physical connection to the outside environment, allowing flux to leak out of the magnet, compromising the shielding.

During this experimental process, we noticed that the field profile slope changed by a few μT/mm every time the magnet was split and closed. The variability of the slope arose from non-parallel splitting, i.e. the magnet pieces initially tended to tilt before completely breaking contact. In this case, the lower part of the yoke touches the upper part on one localized spot along the edge. This redistributes the flux and concentrates it through the contact area, essentially walking the BH curve to the right and decreasing the relative permeability, μ. Even after the magnet is closed, it maintains a state of smaller relative permeability due to the hysteretic behavior of the BH curve. Hence, in the closed state the bottom yoke conducts the magnetic field worse and the flux in the gap is lowered [2].

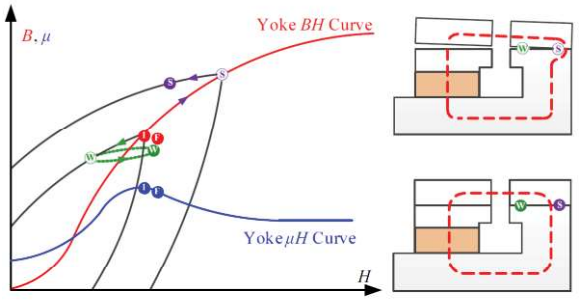

FIGURE 6. Schematic drawing showing the change in the outer part of the yoke before, during, and after opening with an angle. We consider the locations S and W at the small and wide side of the gap on the outer yoke. At the beginning, the magnetic state is given by the point I on the B-H curve. During opening, the point W moves along a minor hysteresis loop to smaller values of B and H. The point S moves along the major curve to a higher value of B and H. After closing, the point W moves almost back to the original point (the solid W). The point on the small side of the wedge moves along a minor loop to a new point (solid S) that has substantial more B. The mean value can be found at the point denoted by F for final point. Overall the μ_r of the yoke has decreased, reducing the flux in the air gap.

However, this new phenomenon proved beneficial for tuning the field and a procedure was developed. (1) The magnet is opened by a little more than 1mm. (2) A 0.5 mm thick shim piece with a size of approximately 5 cm by 5 cm is inserted in the 1mm gap at an azimuthal position α. (3) The magnet is closed. Due to the shim, the magnet closes in a tilted fashion and the iron at the azimuthal position α + 180° is driven to the state with less relative permeability. Steps (1) through (3) are performed a total of six times, where the azimuthal position is advanced by 60° every time. After this, the iron remains at the less permeable state for the entire circumference. [1]

This shimming process is repeatable. We were able to reproduce the shimming procedure several times, yielding an almost identical field profile each time (Fig. 7).

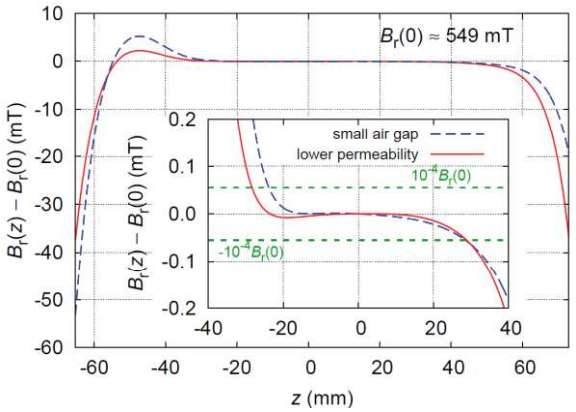

FIGURE 7. Radial flux density as a function of vertical position. The dashed line shows the effects of introducing a small tilt separation.

SHIMMING METHOD APPREHENSIONS

We have two concerns using this shimming method: How stable is the field obtained with this method? Does this process change the azimuthal symmetry of the field? We monitored the field profile for 3 days, taking data every 30 minutes and found the flux density drift in the center of the air gap to be about 2.5 x 10^{-10} T/h, or 0.5 parts per billion per hour. This is enough stability for a watt balance experiment where the flux integral is measured once per hour [2].

The azimuthal variation in the field symmetry proved harder to measure. This can only be done by measuring discrete points around the air gap, meaning the gradiometer coil would be obsolete since it measures the azimuthal integral. Using the hall probe, however, requires precise positioning. Due to the outer yoke design of the magnet, the air gap can be accessed through 12 discrete holes, the middle region of the air gap being 22.5 cm from the top surface. The hall probe must not only be able to reach this location but also be reproducibly inserted in all 12 holes. For example, a 1 mm deviation in the middle of the gap results in a 2.3 mT change. The measurements before and after magnet shimming indicated a similar maximum difference of 1.5 mT. Thus, it is unknown whether or not the uncertainty arises from field inhomogeneity or hall probe positioning error.

CONCLUSION

Both shimming methods have allowed us to achieve the desired field profile uniformity of .01%

(50 uT) over a 50 mm tall section of the air gap. In the end, we chose to shape the field with the method of alternating opening/closing tilt shimming because of higher repeatability and maintaining a closed magnet system.

The magnet has recently been installed in our watt balance. Most of the mechanics of the new watt balance have also been mounted on top of the magnet, inside the vacuum chamber. A handful of velocity mode (the calibration mode of a watt balance experiment to characterize the magnetic field) measurements have already been conducted but no further investigation has been done for uniformity changes. Since uniformity is a larger factor in the weighing mode, we will revisit this topic when we begin taking weighing mode measurements.

REFERENCES

[1] S. Schlamminger, IEEE Trans. Instrum. Meas. 62 1524 (2013).
[2] F. Seifert *et al.* CPEM. submitted for publication (2014).